Density functional study of phosphorus and arsenic clusters using local and nonlocal energy functionals

P. Ballone and R. O. Jones

Citation: The Journal of Chemical Physics **100**, 4941 (1994); doi: 10.1063/1.467213
View online: http://dx.doi.org/10.1063/1.467213
View Table of Contents: http://scitation.aip.org/content/aip/journal/jcp/100/7?ver=pdfcov
Published by the AIP Publishing

Density functional study of phosphorus and arsenic clusters using local and nonlocal energy functionals

P. Ballone and R. O. Jones
Institut für Festkörperforschung, Forschungszentrum Jülich, D-52425 Jülich, Germany

(Received 20 October 1993; accepted 14 December 1993)

Previous calculations of the structures of isomers of phosphorus clusters up to P_{11} (density functional calculations with simulated annealing, local spin density approximation to the exchange-correlation energy) have been extended to arsenic clusters. The structures of As_n clusters are characterized by an almost uniform expansion ($\sim$ 9%) of the corresponding P_n isomers. All cluster isomers have also been studied using a nonlocal, gradient corrected (Becke–Perdew) energy functional. While the structures are almost unchanged, there are significant improvements in the cohesive energies of all clusters. We present a simple picture to show that the improvements arise from contributions both in the atoms and near the "surface" of the clusters.

I. INTRODUCTION

The structures of the many forms of the group Va (group 15) elements phosphorus and arsenic have been of continuing interest for decades. The crystalline forms of phosphorus[1] include puckered layers (black, orthorhombic), long pentagonal tubes containing cage-like P_8 and P_9 groups (Hittorf's violet, monoclinic) and a rhombohedral form related to the structure of α arsenic. Both elements occur as amorphous materials and as solids comprising tetrahedral units (white P, yellow As). Interest in the clusters of these elements has grown following the identification by Martin[2] of the positive ions of P_n up to $n=24$, and the widespread use of arsenic vapor in the epitaxial growth of films of GaAs. Clusters of phosphorus and arsenic have also been studied widely as components of organometallic and other molecules.[3–6]

In recent years an extensive study of different forms of phosphorus has been carried out in our institute. We have used the density functional (DF) formalism,[7] with a local spin density (LSD) approximation for the exchange-correlation energy E_{xc}, combined with molecular dynamics (MD) as proposed by Car and Parrinello.[8] The MD/DF approach has been used for simulations of amorphous (red) phosphorus at 300 K (Ref. 9) and to study, in the liquid state, the polymerization of an assembly of P_4 tetrahedra to a disordered network.[10] In the case of arsenic, it has been applied elsewhere to simulations of the liquid at 1150 K.[11] The method can also be utilized to probe the energy surface of atomic clusters and, by using repeated heating and cooling cycles ("simulated annealing"), to find the minima in the potential energy surfaces and the related structures. We have performed such studies of neutral and charged clusters of phosphorus with up to 11 atoms.[12,13]

The calculations led to some unexpected predictions for the structures of the most stable isomers, and interesting trends as the number of atoms increases. The most stable isomers of P_5, P_6, and P_7, for example, are obtained from the "roof" or "butterfly" structure of P_4 (C_{2v}) by the addition of one, two, and three atoms, respectively. The most stable form of P_8 is not a cube, but a wedge-shaped (C_{2v}) structure analogous to the cuneane isomer of $(CH)_8$.[12] Stable forms of P_9, P_{10}, and P_{11} can be related to this structure by the addition of 1, 2, and 3 atoms along a preferred axis. There are striking similarities in the bond angle distributions in amorphous phosphorus and in P_n clusters with up to 11 atoms.

While the *structures* of clusters and small molecules are given reliably by calculations using a local density approximation for E_{xc}, it is well known that energy differences—such as dissociation and cohesive energies—are less reliable.[7] Both aspects are apparent in the results of more recent calculations of P_n clusters using correlated wave functions. Häser, Schneider, and Ahlrichs[14] have performed calculations on a variety of phosphorus clusters up to P_{28} using Hartree–Fock (HF) calculations and second-order Møller–Plesset (MP2) estimates of the correlation energies, and Janoschek[15] has performed MP4 calculations on isomers of P_6 and P_8. Both sets of calculations support the LSD predictions of the most stable isomers of P_6 and P_8, but the ordering of the isomers showed some differences, and Häser, Schneider, and Ahlrichs[14] found a low-lying isomer of P_{10} that had not been found in the MD/DF work. Furthermore, the MP calculations indicated that two P_4 tetrahedra should be more stable than the cuneane isomer of P_8, while the opposite was found in the LSD calculations.

There have been indications for some time[16] that difficulties in calculating energy differences in local density calculations could be traced to the LSD description of the exchange energy. In seeking improvements, it is natural to include information on the spatial variation of the electron density $n(\mathbf{r})$ using the gradient $\nabla n(\mathbf{r})$:

$$E_{xc}=\int d\mathbf{r}\ f(n(\mathbf{r}),\nabla n(\mathbf{r})). \tag{1}$$

While the systematic development of an appropriate function f around uniform electron gas values is not adequate for most purposes,[7] semi-empirical schemes have achieved satisfactory results in a number of cases.[17] Further work has led to generalized gradient approximations (GGA) for the exchange energy by Perdew and Wang[18] and by Becke,[19] and for the correlation energy by Perdew.[20] The combined approximations of Perdew and Wang (PW) and Becke and Per-

dew (BP) have been studied in some detail in a range of contexts, including the cohesive energy and equilibrium distances in solids,[21,22] molecules,[23–25] and in simulations of metal clusters[26] and hydrogen bonded systems.[27] With a few exceptions,[22] the generalized gradient approximations (GGA) have provided significant improvements over LSD results for energy differences, with only a modest increase in computing requirements.

In the present paper, we extend our previous LSD studies of phosphorus clusters to arsenic, and perform GGA calculations of Becke–Perdew type for both P_n and As_n up to $n=11$. We examine both the bonding trends in these group Va (group 15) elements and the differences brought about by the nonlocal description of E_{xc}. In Sec. II we outline the features of the calculations needed in the present context, we present the results in Sec. III and our discussion and concluding remarks in Sec. IV. A Hartree–Fock configuration interaction study of As_3 to As_6 was published[28] after this work was submitted. The results are discussed below.

II. METHOD OF CALCULATION

In order to facilitate the comparison with our previous work, the LSD calculations on As_n clusters have been performed with the method described in Ref. 12. We use an f.c.c. unit cell with lattice constant 30 a.u., a plane wave basis set with energy cutoff 5.3 a.u., and a single point ($k=0$) in the Brillouin zone. The electron-ion interaction is described by the nonlocal pseudopotential of Bachelet, Hamann, and Schüter,[29] using the d component of the potential as the reference local part ("sp nonlocality"). The phosphorus and arsenic clusters were calculated in parallel, so that structural information determined for one element could be used for the other.

The use of a nonlocal form for E_{xc} means that a new pseudopotential must be generated. We have derived this from an atomic calculation with gradient corrections using the prescription of Hamann, Schlüter, and Chiang.[30] The cutoff radii were close to those used in Ref. 29. More details of the pseudopotential construction, including the precise form of the exchange-correlation energy and potential, are given in Ref. 25. Its transferability, as measured by comparisons of all-electron and pseudopotential energies of excited atomic configurations, is very similar to that of the LSD pseudopotentials.

The pseudo-atom energy used to computed the cohesive energy has been determined by a spin polarized atomic program. To save computer time, we have not included spin polarization in the cluster calculations. Since the smallest clusters with unpaired spins (P_3 and As_3) already contain 15 electrons, this effect is small. The plane wave basis has been tested on the homonuclear diatomic molecules, and the binding energy and cohesive energies are well converged with a cutoff of 17.5 a.u. for phosphorus and 12 a.u. for arsenic. All calculations were performed with an f.c.c. unit cell with lattice constants of 30 a.u. and 36 a.u. for P and As, respectively, implying about 11500 plane waves in the expansion of the single particle orbitals for each element. These tests confirm that essential input into the calculations, like the basis set truncation or the use of periodic boundary conditions (implying a small interaction between clusters in neighboring cells) can easily be checked and are much less important than the approximations used for E_{xc}.

TABLE I. Cohesive energies (binding energies per atom, eV) of isomers of P_n and As_n clusters.

	GC	LSD		GC	LSD
P_2	2.61	3.08	As_2	2.16	2.58
$P_3(C_{2v})$	2.52	3.16	$As_3(C_{2v})$	2.25	2.70
$P_4(T_d)$	3.17	3.90	As_4 (T_d)	2.91	3.38
P_4 (C_{2v})	2.68	3.35	As_4 (C_{2v})	2.42	2.87
P_5 (C_{2v})	2.87	3.62	As_5 (C_{2v})	2.63	3.15
P_6 (C_{2v})	3.06	3.79	As_6 (C_{2v})	2.77	3.27
P_6 (D_{3h})	3.02	3.76	As_6 (D_{3h})	2.76	3.28
P_7 (C_s)	3.03	3.82	As_7 (C_s)	2.77	3.31
P_8 (C_{2v})	3.15	3.96	As_8 (C_{2v})	2.88	3.43
P_8 (D_{2h})	3.09	3.86	As_8 (D_{2h})	2.84	3.36
P_8 (O_h)	2.97	3.74	As_8 (O_h)	2.71	3.27
P_9 (C_s) [a]	3.09	3.92	As_9 (C_s)[a]	2.82	3.40
P_9 (C_s) [b]	3.09	3.90	As_9 (C_s)[b]	2.81	3.37
P_9 (C_s) [c]	3.08	3.89	As_9 (C_s)[c]	2.80	3.36
P_{10} (C_s)	3.19	4.03	As_{10} (C_s)	2.92	3.50
P_{10} (C_{2v})	3.20	4.02	As_{10} (C_{2v})	2.91	3.48
P_{11} (C_2)	3.16	4.02	As_{11} (C_2)	2.89	3.49
P_{11} (C_s)	3.16	4.01	As_{11} (C_s)	2.89	3.47

[a]Figure 3(a) of Ref. 13.
[b]Figure 3(b) of Ref. 13.
[c]Figure 3(c) of Ref. 13.

III. RESULTS

The structures and binding energies of phosphorus clusters calculated using the LSD approximation for E_{xc} are given in Refs. 12 and 13, and the reader is referred to these papers for details and figures of all the isomers calculated. We focus in this section on the analogous results for arsenic clusters, and on the effects of gradient corrections on P_n and As_n. The LSD and GC values of the cohesive energy E_{coh} (the total binding energy per atom) are given in Table I for the most stable of the clusters we have studied.

A. LSD results for arsenic clusters

As in most elements, the best studied cluster of arsenic is the homonuclear diatomic molecule As_2, and in Table II we compare the results of some recent calculations[31–34] with experimental spectroscopic parameters.[35] We have a very simi-

TABLE II. Spectroscopic constants for $^1\Sigma_g^+$ state of As_2.

Method	r_e (a.u.)	ω_e cm^{-1}	D_e (eV)
MCSCF+FOCI[a]	4.09	394	2.71
LSD, LCGTO[b]	3.940	446	4.76
CCSD[c]	3.982	447	3.10
MRD-CI[d]	4.12	430	2.54
LSD, this work	3.89	423	5.17
Experiment[e]	3.973	429.55	3.96

[a]Multiconfiguration SCF + first order configuration interaction (Ref. 31).
[b]LSD calculations with Gaussian orbitals (Ref. 32).
[c]Coupled cluster calculations with single and double excitations (Ref. 33).
[d]Multiple reference determinant configuration interaction (Ref. 34).
[e]Reference 35.

lar picture to that in P_2,[12] in that the equilibrium separation and vibration frequency are given satisfactorily by all methods, and the dissociation energy is underestimated by calculations using correlated wave functions and overestimated by density functional calculations with the LSD approximation. The overestimate in the present calculations (1.2 eV) is similar to that found in P_2 (1.1 eV).[12]

The arsenic trimer has been identified in gas phase charge transfer reactions,[36] and CI calculations have been performed by Igel–Mann *et al.*[28] and Balasubramanian *et al.*[37] In the D_{3h} structure (bond angle 60°), the highest occupied molecular orbital is doubly degenerate (e'') and contains a single electron. Jahn–Teller distortions to C_{2v} structures with bond angles greater and less than 60° are possible, and both occur in P_3 and As_3. The D_{3h} structure ($^2E''$) has a bond length of 4.40 a.u. and the C_{2v} structures are less than 0.1 eV more stable. The geometry of the $^2B_1$ state (bond angle α=55.6°, 4.21 a.u., 4.51 a.u.) is in excellent agreement with that found by Igel-Mann, Stoll, and Preuss[28] (56°, 4.18 a.u., 4.48 a.u.), and the same applies to the $^2A_2$ state [(65.4°, 4.29 a.u., 4.64 a.u.) and (65°, 4.28 a.u., 4.60 a.u.), respectively]. The energies of the two states are virtually degenerate, the latter being 0.01 eV more stable in the present calculations. The same ordering is found by Balasubramanian, Sumathi, and Dai[37] (ΔE=0.05 eV), although their bond lengths are ~4%–5% longer.

The arsenic tetramer has received considerable attention, since it is the most prominent component of arsenic vapor between 400 and 850 K,[38,39] and high resolution photoelectron spectroscopy has been performed on both As_2[40,41] and As_4.[41,42] Gas electron diffraction measurements of Morino, Ukaji, and Ito[43] indicate that the tetramer is tetrahedral, with an internuclear separation of 4.602 ± 0.008 a.u. LSD calculations lead to 4.613 a.u.[32] and 4.56 a.u. (this work), and configuration interaction calculations give 4.73 a.u.[34] and 4.67 a.u.[28] The equilibrium between As_2 and As_4 has been studied in detail in the gas phase by Murray, Pupp, and Pottie.[44] The enthalpy of the reaction $As_4(g) \rightleftharpoons As_2(g)$ was found to be 2.35 eV, compared with the LSD-GTO value[32] of 3.23 eV and the CI result of 1.79 eV.[34] The result of the present calculation (3.17 eV) is consistent with the former, and is a further instance of an overestimate of binding energies by the LSD approximation.

Our previous calculations on P_4 showed that there is a "roof" or "butterfly" (C_{2v}) isomer, with an energy substantially (2.1 eV) above that of the tetrahedron. The C_{2v} isomer is interesting, because it has a very large basin of attraction and is the basis for the most stable isomers found for P_5, P_6, and P_7. It is also well known as a component of phosphane molecules[6] and occurs as As_4 as a ligand in organometallic molecules.[3,5] Apart from a scaling factor, the calculated As_4 "roof" structure (triangles with two sides of 4.43 a.u. and a common side of 4.84 a.u., with a dihedral angle of 34.9 °) is very similar to that of the P_4 isomer (4.04 a.u., 4.45 a.u., 32.8 °), as is the energy difference (2.0 eV) above the T_d structure.

In As_2, As_3, and the above two isomers of As_4 the As–As bonds are ~ 9% longer than the corresponding P–P bonds. A remarkably uniform scaling of this amount (between 8% and 10%) is found in all the cluster isomers discussed in Refs. 12 and 13, so that the structural trends found in P_n clusters are also found in As_n clusters. An example is the change in the P_4 and As_4 "roof" components of the low-lying isomers of P_5–P_8. The benzvalene form of As_6, with the central bond of the roof opened, has been found as a component of $(Cp''_2Th)_2(\mu\text{-}\eta^{3:3}\text{-}As_6)$.[45] A scaling between the geometries found for phosphorus and arsenic clusters is also found in LSD calculations we have now performed for the C_{2v} isomer of P_{10} found by Häser, Schneider, and Ahlrichs.[14] The bond lengths and bond angles are shown in Table III, and it is striking that almost all bond angles differ by less than 1° between the P and As forms.

TABLE III. Bond lengths d (a.u.) and bond angles α in C_s and C_{2v} isomers of P_{10} and As_{10}.

	P_{10} (C_s) [a]	As_{10} (C_s)		P_{10} (C_{2v})	As_{10} (C_{2v})
d_{12}	4.17	4.56	d_{12}	4.21	4.61
d_{23}	4.15	4.51	d_{23}	4.21	4.60
d_{34}	4.29	4.69	d_{13}	4.20	4.59
d_{45}	4.21	4.58	d_{34}	4.15	4.55
d_{56}	4.16	4.51	d_{45}	4.15	4.54
d_{67}	4.37	4.85	α_{213}	60.1	59.8
d_{78}	4.26	4.62	α_{132}	60.2	60.3
d_{89}	4.09	4.50	α_{321}	59.6	59.9
$d_{1,10}$	3.92	4.35	α_{234}	108.0	107.0
α_{123}	107.8	108.0	α_{134}	104.8	105.4
α_{234}	97.6	97.3	α_{345}	103.6	103.7
α_{345}	106.7	106.7	α_{346}	96.4	93.7
α_{456}	60.4	60.5			
α_{546}	59.1	58.9			
α_{458}	101.3	101.7			
α_{672}	94.4	92.5			
α_{721}	73.5	70.0			
α_{723}	102.1	102.3			
$\alpha_{21,10}$	107.3	107.0			

[a]After Ref. 12, with two corrections.

While P_n and As_n show remarkably similar structures, there are some differences in the relative energies of the different isomers. In P_{10}, for example, the most stable form found in our earlier LSD calculations [C_s, Fig. 1(a)] is slightly [ΔE=0.14 eV] more stable than the C_{2v} form [Fig. 1(b)], while the energy difference is larger [ΔE=0.21 eV] in As_{10}. Häser, Schneider, and Ahlrichs find that the C_{2v} isomer in P_{10} is more stable by a small amount (0.058 eV). With the exception of the hexamer, LSD calculations predict that the most stable isomers are the same in P_n and As_n up to n=11. As noted in Ref. 12, the prismane (D_{3h}) structure in As_6 is slightly (0.06 eV) more stable than the benzvalene (C_{2v}) isomer. The D_{3h} structure was found by Igel-Mann, Stoll, and Preuss[28] to be more stable than the hexagonal (D_{6h}) and octahedral (O_h) forms. We discuss the relative energies of the different isomers in more detail below, where we show that the incorporation of gradient corrections in E_{xc} leads to changes in both P_n and As_n clusters.

B. Structures of P_n and As_n clusters with gradient corrections

The results of the LSD calculations described in Ref. 12 and in Sec. III A are consistent with the picture usually

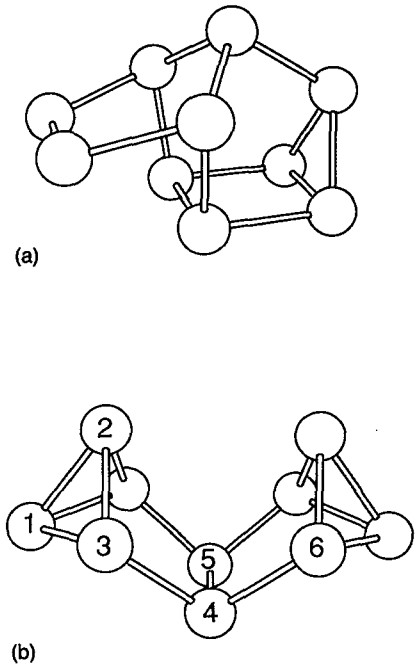

FIG. 1. Two low-lying isomers of P_{10}: (a) C_s, (b) C_{2v}.

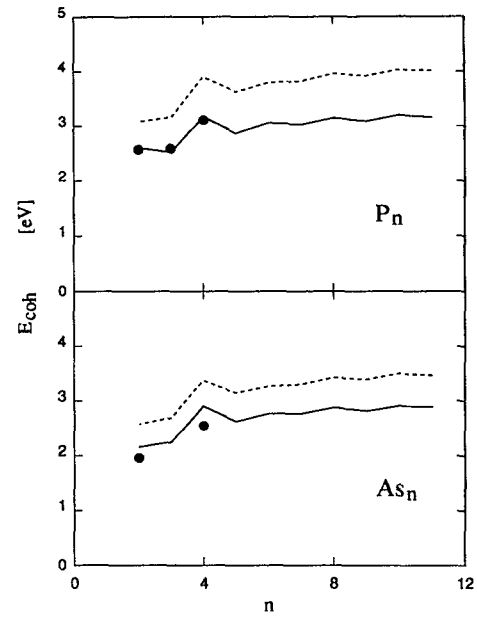

FIG. 2. Cohesive energies (binding energies per atom) of P_n and As_n clusters. Broken curves: LSD calculations, full curves: GC calculations, circles: experimental values.

found in sp-bonded molecules.[7] Where they are known, the experimental geometries and the variations in energy around the corresponding minima—as measured by vibration frequencies—are reproduced well by LSD calculations.[46] On the other hand, binding and cohesive energies E_{coh} for P_2, P_3, P_4, As_2, and As_4 are systematically overestimated. This problem is significant if one focuses on the relative stabilities of different clusters, and even more important in the calculation of fragmentation energies. We now study the effect of gradient corrections in E_{xc} on such energy differences.

Previous experience has shown that, while GC can lead to significant changes to LSD energy differences, the structures derived from the two Born–Oppenheimer surfaces are very similar. This is not surprising, since the local coordination and the preferred bond lengths and angles are already described well by LSD calculations. For this reason, we have not repeated the extensive search for the stable (and metastable) geometries performed in Ref. 12 and in Sec. III A, but have started from the LSD atomic positions and have then minimized the electronic energy according to the GC functional. The atomic positions are then allowed to relax to the nearest local energy minimum by alternating MD and quenches. We performed an extended MD simulation in the case of P_8, but did not find any structure that had not been found in the LSD work.

For each LSD structure we found a closely related GC structure that differed from the former by an almost homogeneous expansion of bond lengths by $\sim$ 1%. In P_2, for example, the equilibrium internuclear separation r_e^{GC} is 3.60 a.u., compared with r_e^{LSD} of 3.56 a.u. and the experimental value of 3.578 a.u.,[35] and r_e increases in P_4 (T_d) from 4.18 a.u. to 4.22 a.u., compared with the measured value of 4.2006 a.u.[47] The energetic ordering of the isomers is also very similar to that found in the LSD calculations, with a change in relative stability only in As_6 and P_{10} for isomers rather close in energy. In the case of P_{10}, the inclusion of gradient corrections means that the C_{2v} isomer [Fig. 1(b)] is 0.10 eV more stable than the C_2 isomer [Fig. 1(a)], in agreement with the results (Hartree–Fock with second order Møller–Plesset corrections) of Häser, Schneider, and Ahlrichs.[14] The GC energy difference between the most stable (benzvalene) and the prismane isomers of P_6 (0.23 eV) is less than the value (0.64 eV) found by MP2 (Ref. 14) and MP4(SDQ) (Ref. 15) calculations.

While the structural parameters and the energetic ordering of the isomers are very similar in both LSD and GS calculations, Table I shows that there are significant differences in the cohesive energies E_{coh} for P_n and As_n clusters. A comparison with the experimental values of E_{coh} in P_2, P_3, and P_4 [2.52, 2.59, 3.11 eV, respectively] indicates that GC provide a major improvement over LSD calculations in small phosphorus clusters. The improvements in arsenic clusters are less pronounced (the measured values of E_{coh} in As_2 and As_4 are 1.97 and 2.55 eV, respectively) and are more in line with the results of previous tests of gradient corrections. The calculated and experimental cohesive energies are shown in Fig. 2.

Differences in cohesive energies are reflected, of course, in changed fragmentation energies. Of particular interest in this context are the cluster energies with respect to the particularly strongly bound P_4 and As_4 tetrahedra. In agreement with HF calculations with MP corrections, gradient corrections reverse the LSD result on the the relative stability of P_8 and 2 P_4, predicting the former to be less stable. The structure determined by LSD simulated annealing, however, has a large barrier to fragmentation, and $\sim$ 8000 MD time

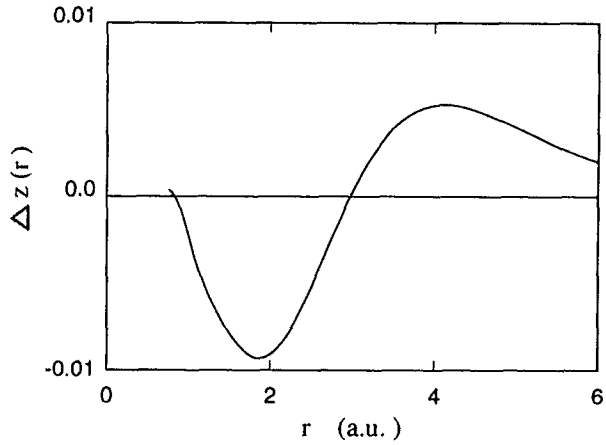

FIG. 3. Plot of $\Delta z(r)=4\pi r^2(n^{GC}(r)-n^{LSD}(r))$ for the P pseudoatom. Atomic units.

steps (total time of 1.4 ps) at 500 K were not sufficient to observe the decay of this cluster.

IV. DISCUSSION AND CONCLUSIONS

In the first part of the paper we extended our previous LSD study of isomers of phosphorus clusters to clusters of arsenic with up to 11 atoms. While there were small changes in the ordering of the energies of the isomers of some clusters, we found that the structures of As_n clusters are generally related to the corresponding P_n structures by an expansion of $\sim 9\%$. This is consistent with the atomic radii (and the atomic valence orbital functions) found for these elements in a study of molecules containing elements of groups Va and VIa (groups 15 and 16).[48]

We then studied the effect of using gradient corrections to modify the LSD approximation for the exchange-correlation energy, by performing calculations for both P_n and As_n clusters. The inclusion of gradient corrections has a negligible effect on the structures of the clusters, but it reduces substantially the LSD estimate of the cohesive energy per atom $E_{coh}(n)$ and improves the agreement with available experimental data. In Fig. 2 we show that the two approximations lead to approximately parallel plots of E_{coh} as a function of n for both P_n and As_n clusters, but a size dependence is also evident. The effect of gradient corrections is smallest in the dimer, and increases with increasing n. We shall now discuss these points in more detail.

It is well known that LSD values of atomic total energies $E_{tot}(1)$ lie above the exact values.[7,25] The error per atom is smaller in sp-bonded molecules and solids, so that E_{coh} is overestimated. Nonlocal functionals, such as generalized gradient approximations, generally lead to improved values of E_{xc} and $E_{tot}(1)$, and therefore to better estimates of E_{coh}. While improved atomic energies alone do not explain the size dependence evident in Fig. 2, we now show that an analysis of the valence charge density shows that the observed behavior is plausible.

In Fig. 3 we show $\Delta z(r)=4\pi r^2(n^{GC}(r)-n^{LSD}(r))$ for the P pseudoatom, neglecting small amplitude oscillations in the core region. The corresponding curve for As is very similar. Δz has two main components: a negative contribution in the region $1<r<2.8$ a.u., where most of the valence charge is located, and a positive tail. Charge transfer in this direction reflects the increased attraction of the GC potential outside the core. As shown in Fig. 4 for the dimer, the corresponding plot for P clusters is close to a superposition of the atomic picture: The effect of gradient corrections is to transfer charge from the region around each atom ($1<r<2.8$) to the outer region of the cluster. It is natural to interpret the two regions as leading to "atomic" and "surface" contributions to the cohesive energy difference ΔE_{coh}.

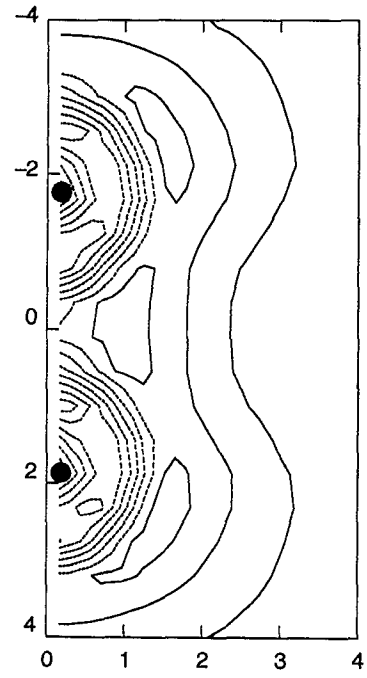

FIG. 4. Contour plot of $\Delta z(\mathbf{r})$ for P_2. Positive contours are shown by full curves, zero and negative contours by dashed curves. The contour interval is 0.004 (a.u.).

This suggests the following relation between the LSD and GC values for the total energy of a single atom:

$$E_{tot}^{GC}(1)=E_{tot}^{LSD}(1)-\alpha-4\pi r_0^2\beta \ , \tag{2}$$

where r_0 is an appropriate scale for the atomic radius, and the last term represents the surface contribution. We then have

$$E_{tot}^{GC}(n)=E_{tot}^{LSD}(n)-\alpha n-4\pi r_0^2\,\beta n^{2/3} \tag{3}$$

and

$$\frac{1}{n}(E_{tot}^{GC}(n)-n\,E_{tot}^{GC}(1))=\frac{1}{n}(E_{tot}^{LSD}(n)-nE_{tot}^{LSD}(1)) + 4\pi r_0^2\beta(1-n^{-1/3}) \ ,$$

so that

$$E_{coh}^{GC}(n)=E_c^{LSD}(n)+k(1-n^{-1/3}). \tag{4}$$

To test this relation we show in Fig. 5 $E_{coh}^{GC}(n)-E_{coh}^{LSD}(n)$ as a function of $n^{-1/3}$. The full curve is a linear fit to the nu-

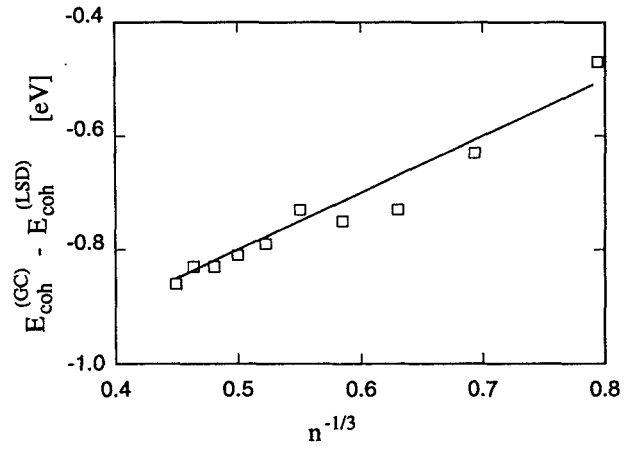

FIG. 5. Difference between cohesive energies E_{coh} calculated with GC and LSD approximations plotted against $n^{-1/3}$.

merical results, and reproduces the behavior of the cohesive energy differences satisfactorily over the range of n studied here.

The present work has provided a further test of the application of density functional calculations to molecules, both with the local spin density approximation and with gradient corrections. Our findings are consistent with those of previous tests, which showed that the equilibrium geometries are given reliably by both schemes, but that the latter give improved dissociation (or cohesion) energies. Since both are computationally much less intensive than those methods of quantum chemistry that focus on correlated wave functions, they provide useful complements to them. It would be very interesting to expand the data base of molecules for which generalized gradient approximations (GGA) have been tested, as this would enable us to understand better the applicability and limitations of the approach. It should be noted that GGA of the form used here cannot reproduce simultaneously the asymptotic form of both the exchange energy density and the exchange potential of finite systems.[49] These limits are, however, not essential to obtain reliable exchange energies,[49] which can therefore be obtained from a variety of approximate forms.

ACKNOWLEDGMENTS

We thank D. J. W. Geldart and G. Seifert for helpful discussions, and T. P. Martin, U. Näher, and O. J. Scherer for experimental results prior to publication. The calculations were performed on Cray computers of the Forschungszentrum Jülich and the German Supercomputer Center (HLRZ).

[1] J. Donohue, *The Structures of the Elements* (Wiley, New York, 1974), Chap. 8.
[2] T. P. Martin, Z. Phys. D **3**, 211 (1986). Measurements on phosphorus clusters P_n have now been extended well beyond n=6000 (T. P. Martin and U. Näher, private communication).
[3] O. J. Scherer, Angew. Chem. **102**, 1137 (1990); Angew. Chem. Int. Ed. Engl. **29**, 1104 (1990).
[4] A. J. DiMaio and A. L. Rheingold, Chem. Rev. **90**, 169 (1990).
[5] O. J. Scherer, K. Pfeiffer, and G. Wolmershäuser, Chem. Ber. **125**, 2367 (1992).
[6] M. Baudler and K. Glinka, Chem. Rev. **93**, 1623 (1993).
[7] For a review, see R. O. Jones and O. Gunnarsson, Rev. Mod. Phys. **61**, 689 (1989).
[8] R. Car and M. Parrinello, Phys. Rev. Lett. **55**, 2471 (1985).
[9] D. Hohl and R. O. Jones, Phys. Rev. B **45**, 8995 (1992) (amorphous P).
[10] D. Hohl and R. O. Jones (to be published) (liquid P).
[11] X.-P. Li, P. B. Allen, R. Car, M. Parrinello, and J. Q. Broughton, Phys. Rev. B **41**, 3260 (1990).
[12] R. O. Jones and D. Hohl, J. Chem. Phys. **92**, 6710 (1990) (clusters up to P_8).
[13] R. O. Jones and G. Seifert, J. Chem. Phys. **96**, 7564 (1992) (clusters up to P_{11}).
[14] M. Häser, U. Schneider, and R. Ahlrichs, J. Am. Chem. Soc. **114**, 9551 (1992).
[15] R. Janoschek, Chem. Ber. **125**, 2687 (1992).
[16] See, for example, O. Gunnarsson and R. O. Jones, Phys. Rev. B **31**, 7588 (1985).
[17] D. C. Langreth and M. J. Mehl, Phys. Rev. B **28**, 1809 (1983).
[18] J. P. Perdew and Y. Wang, Phys. Rev. B **33**, 8800 (1986).
[19] A. D. Becke, Phys. Rev. A **38**, 3098 (1988).
[20] J. P. Perdew, Phys. Rev. B **33**, 8822 (1986); **34**, 7406(E) (1986).
[21] P. Bagno, O. Jepsen, and O. Gunnarsson, Phys. Rev. B **40**, 1997 (1989) (iron series elements); J. P. Perdew, J. A. Chevary, S. H. Vosko, K. A. Jackson, M. R. Pedersen, D. J. Singh, and C. Fiolhais, Phys. Rev. B **46**, 6671 (1992) (atoms, hydrocarbon molecules, alkali metals).
[22] A. García, C. Elsässer, J. Zhu, S. G. Louie, and M. L. Cohen, Phys. Rev. B **46**, 9829 (1992) (Al, Si, Ge, GaAs, Nb, Pd).
[23] A. D. Becke, J. Chem. Phys. **96**, 2155 (1992) (55 small molecules).
[24] B. G. Johnson, P. M. W. Gill, and J. A. Pople, J. Chem. Phys. **97**, 7846 (1992) (32 small molecules).
[25] G. Ortiz and P. Ballone, Phys. Rev. B **43**, 6376 (1991) (homonuclear dimers); G. Ortiz, Phys. Rev. B **45**, 11328 (1992) (Si, Ge, GaAs).
[26] P. Delaly, P. Ballone, and J. Buttet, Phys. Rev. B **45**, 3838 (1992) (Mg microclusters).
[27] K. Laasonen, F. Csajka, and M. Parrinello, Chem. Phys. Lett. **194**, 172 (1992) (water dimer); C. Lee, D. Vanderbilt, K. Laasonen, R. Car, and M. Parrinello, Phys. Rev. Lett. **69**, 462 (1992) (high pressure phases of ice).
[28] G. Igel-Mann, H. Stoll, and H. Preuss, Mol. Phys. **80**, 325 (1993).
[29] G. B. Bachelet, D. R. Hamann, and M. Schlüter, Phys. Rev. B **26**, 4199 (1982).
[30] D. R. Hamann, M. Schlüter, and C. Chiang, Phys. Rev. Lett. **43**, 1494 (1979).
[31] K. Balasubramanian, J. Mol. Spectrosc. **121**, 465 (1987).
[32] J. Andzelm, N. Russo, and D. R. Salahub, Chem. Phys. Lett. **142**, 169 (1987).
[33] G. E. Scuseria, J. Chem. Phys. **92**, 6722 (1990).
[34] U. Meier, S. D. Peyerimhoff, and F. Grein, Chem. Phys. **150**, 331 (1991).
[35] K. P. Huber and G. Herzberg, *Molecular Spectra and Molecular Structure. Vol. IV Constants of Diatomic Molecules* (Van Nostrand, New York, 1979).
[36] J. A. Zimmermann, S. B. H. Bach, C. H. Watson, and J. R. Eyler, J. Phys. Chem. **95**, 98 (1991).
[37] K. Balasubramanian, K. Sumathi, and D. Dai, J. Chem. Phys. **95**, 3494 (1991).
[38] J. S. Kane and J. H. Reynolds, J. Chem. Phys. **25**, 342 (1956).
[39] J. M. Dyke, S. Elbel, A. Morris, and J. C. H. Stevens, J. Chem. Soc., Faraday Trans. 2 **82**, 637 (1986).
[40] L.-S. Wang, Y. T. Lee, D. A. Shirley, K. Balasubramanian, and P. Feng, J. Chem. Phys. **93**, 6310 (1990).
[41] R. K. Yoo, B. Ruscic, and J. Berkowitz, J. Chem. Phys. **96**, 6696 (1992).
[42] L. S. Wang, B. Niu, Y. T. Lee, D. A. Shirley, E. Ghelichkhani, and E. R. Grant, J. Chem. Phys. **93**, 6318, 6327 (1990).
[43] Y. Morino, T. Ukaji, and T. Ito, Bull. Chem. Soc. Jpn. **39**, 64 (1966).
[44] J. J. Murray, C. Pupp, and R. F. Pottie, J. Chem. Phys. **58**, 2569 (1973).
[45] O. J. Scherer and J. Schulze (to be published). Cp'' denotes $C_5H_3(t\text{-}Bu)_2$-1,3.
[46] Coordinates of structures found in the LSD calculations can be obtained on request from R.O. Jones.
[47] N. J. Brassington, H. G. M. Edwards, and D. A. Long, J. Raman Spectrosc. **11**, 346 (1981).
[48] R. O. Jones and G. Seifert, J. Chem. Phys. **96**, 2942 (1992).
[49] E. Engel, J. A. Chevary, L. D. Macdonald, and S. H. Vosko, Z. Phys. D **23**, 7 (1992).